





## Varying influence of phytoplankton biodiversity and stoichiometric plasticity on bulk particulate stoichiometry across ocean basins

Michael W. Lomas<sup>1</sup><sup>✉</sup>, Steven E. Baer<sup>2</sup>, Celine Mouginot<sup>3</sup>, Kristina X. Terpis<sup>4</sup>, Debra A. Lomas<sup>1</sup>, Mark A. Altabet<sup>5</sup> & Adam C. Martiny<sup>3,6</sup>

Concentrations and elemental ratios of suspended particulate organic matter influence many biogeochemical processes in the ocean, including patterns of phytoplankton nutrient limitation and links between carbon, nitrogen and phosphorus cycles. Here we present direct measurements of cellular nutrient content and stoichiometric ratios for discrete phytoplankton populations spanning broad environmental conditions across several ocean basins. Median cellular carbon-to-phosphorus and nitrogen-to-phosphorus ratios were positively correlated with vertical nitrate-to-phosphate flux for all phytoplankton groups and were consistently higher for cyanobacteria than eukaryotes. Light and temperature were inconsistent predictors of stoichiometric ratios. Across nutrient-rich and phosphorus-stressed biomes in the North Atlantic, but not in the nitrogen-stressed tropical North Pacific, we find that a combination of taxonomic composition and environmental acclimation best predict bulk particulate organic matter composition. Our findings demonstrate the central role of plankton biodiversity and plasticity in controlling linkages between ocean nutrient and carbon cycles in some regions.

<sup>1</sup>Bigelow Laboratory for Ocean Sciences, East Boothbay, ME, USA. <sup>2</sup>Corning School of Ocean Studies, Maine Maritime Academy, Castine, ME, USA.

<sup>3</sup>Department of Earth System Science, University of California at Irvine, Irvine, CA, USA. <sup>4</sup>Department of Biological Sciences, University of Rhode Island, Kingston, RI, USA. <sup>5</sup>School of Marine Science and Technology, University of Massachusetts Dartmouth, New Bedford, MA, USA. <sup>6</sup>Department of Ecology and Evolution, University of California at Irvine, Irvine, CA, USA. ✉email: [mlomas@bigelow.org](mailto:mlomas@bigelow.org)

Marine phytoplankton elemental stoichiometry has received a significant amount of new attention over the past decade from both observational and theoretical points of view, given the central role of stoichiometric ratios in understanding global patterns in primary production, carbon export, and interconnectivity between trophic levels<sup>1,2</sup>. Eight decades ago Alfred C. Redfield observed that the mean ratio of sestonic particulate organic carbon (C) to nitrogen (N) to phosphorus (P) was similar across ocean regions at 106:16:1, albeit with wide ranges in values, and was similar to the dissolved inorganic nutrient ratios in the deep ocean. Redfield hypothesized that this global mean state was owing to the remineralization of sinking particulate material derived from the stoichiometric preferences of phytoplankton<sup>3</sup> but did not rule out regional patterns in phytoplankton community selection and/or nitrogen cycle feedbacks<sup>4</sup>. As data have accumulated, consistent spatial patterns of deviation from the Redfield Ratio have emerged, although the underlying mechanisms continue to be debated.

Spatial variability in the average taxonomic composition of natural phytoplankton populations has been hypothesized as an important driver of observed patterns in bulk particulate stoichiometry<sup>5,6</sup>. For example, diatoms<sup>7,8</sup>, which thrive in nutrient-rich environments, commonly display N:P ratios lower than the Redfield Ratio, whereas in contrast, cyanobacteria, which thrive in nutrient-poor environments, commonly display N:P ratios greater than the Redfield Ratio in culture<sup>9</sup>. C:N ratios, in contrast, range much more narrowly among taxa. While broad taxonomically linked stoichiometric ratios are observed<sup>5</sup>, they are not constant, as within a given phytoplankton taxa phenotypic acclimation to nutrient conditions does occur<sup>10,11</sup>. Similarly, in the subtropical N. Atlantic it has been shown that specific phytoplankton taxa from natural populations have different stoichiometric ratios as a function of depth at the same station<sup>5</sup>. Sharoni and Halevy<sup>6</sup>, based on a meta-analysis of field data, concluded that phytoplankton community composition, using “optimum-growth” mean cellular stoichiometries associated with each taxonomic group, was a better predictor of bulk particulate N:P ratios than a nutrient concentration acclimation model. Reaching a different conclusion, Galbraith and Martiny<sup>12</sup> observed a robust relationship between ambient phosphate concentrations and bulk particulate N:P ratios, which was mechanistically linked to plasticity in the ability of certain phytoplankton to modulate phosphorus content. The results of these two studies are not mutually exclusive, owing to the covariance of elevated nutrient concentrations and phytoplankton communities dominated by diatoms<sup>13</sup>.

In assessing phytoplankton elemental stoichiometry, measurement of bulk POM ratios leads to biases of varying degrees

through the inclusion of heterotrophic and detrital particles<sup>14–16</sup>. The inclusion of detrital particles can lead to elevated POM ratios, in nutrient-depleted regions<sup>17</sup>, independent of the living phytoplankton community. Latitudinal patterns of elevated POM ratios in the tropics and lower ratios in polar waters could thus result from the additive patterns of decreasing relative contribution of detrital particles and increasing prevalence of diatoms from the equator to the poles. Although studies have concluded that phytoplankton biodiversity is a more important driver of POM composition<sup>5–8,18</sup>, these studies, except for those of Martiny et al.<sup>5</sup> and Baer et al.<sup>18</sup>, have only correlated patterns in biodiversity with bulk POM composition. Further, disentangling the phytoplankton community from phenotypic plasticity within a taxonomic group is an extant challenge, and this study presents direct observational data focused on this challenge. This study addresses the following questions. What is the variability in element contents and stoichiometric ratios for specific phytoplankton populations across ocean regions? Does environmental forcing modulate the observed stoichiometric ratios within a taxonomic group? Do shifts in biodiversity contribute to variation in bulk C:N:P of marine communities?

## Results and discussion

**Cellular macronutrient contents.** Only in the North Atlantic have studies directly measured stoichiometric ratios in phytoplankton taxa physically separated from natural populations. Results highlighted the first-order role of phytoplankton biodiversity for determining variations in elemental ratios<sup>5,18</sup>. In contrast, in the eastern Indian Ocean, with muted variability in phytoplankton biodiversity, relative to the North Atlantic, studies of bulk POM stoichiometry identified an important role for nutrient supply, using nutricline depth as a proxy<sup>19</sup>. Coupled trait-based/remote-sensing input models applied to the global ocean reach equally diverse conclusions of the importance of biodiversity<sup>6</sup> versus nutrient inputs when applied to the global ocean<sup>15</sup>. Here, we present a data set collected from several major ocean basins and a range of environments (Fig. 1) where we have used fluorescence-activated cell sorting to isolate populations of important picocyanobacteria, *Prochlorococcus* and *Synechococcus*, and operationally defined picoeukaryotic phytoplankton for subsequent analysis of their elemental macronutrient content and calculated stoichiometric ratios. The data set comprises results from samples sorted both live (immediately at sea) and those fixed and sorted in the shore-side laboratory, as the difference between them in paired samples was found to be acceptably small (Supplementary Figure 1). For a given element, cellular contents generally spanned a similar range between different biogeographic

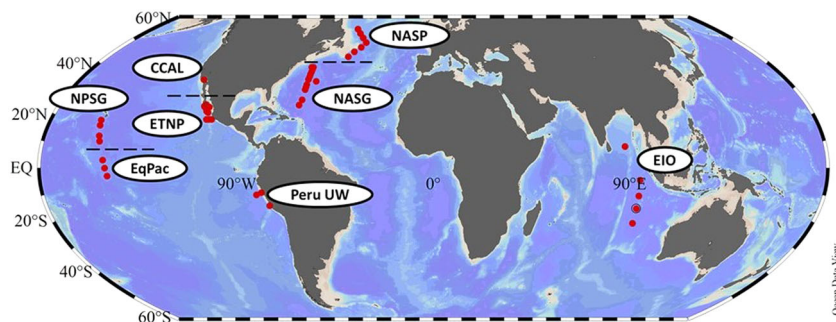


**Fig. 1 Map of stations from which samples were collected and cell-sorted to quantify cellular macronutrient content.** Circled abbreviations represent the regions: North Atlantic Subpolar (NASP), North Atlantic Subtropical Gyre (NASG), Coastal California (CCAL), Eastern Tropical North Pacific (ETNP), North Pacific Subtropical Gyre (NPSG), Equatorial Pacific (EqPac), Eastern Indian Ocean (EIO), and the Peru upwelling region (Peru UW). Specific cruise details can be found in Supplementary Table 1. Dashed lines denote the separation between stations in neighboring regions. Map created in Ocean Data View (Schlitzer, R., Ocean Data View, <http://odv.awi.de>, 2014).

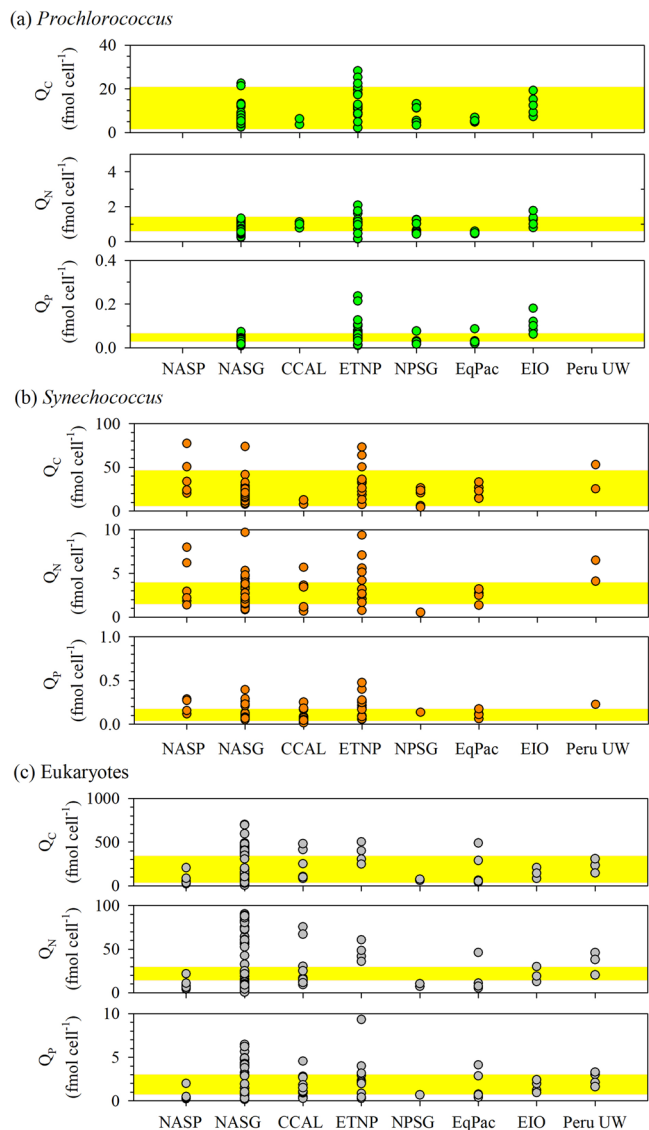


**Fig. 2** Biogeographical distribution of phytoplankton carbon, nitrogen, and phosphorus contents. (a) *Prochlorococcus*, (b) *Synechococcus*, and (c) eukaryotes, and in each, the upper figure is the cellular elemental quota of carbon ( $Q_C$ ), the middle figure is the cellular elemental quote of nitrogen ( $Q_N$ ) and the lower figure is the cellular elemental quota of phosphorus ( $Q_P$ ). Regions denoted on the x axis are as defined in Fig. 1. For *Prochlorococcus*, there are no data for NASP and Peru UW as populations were either not present, or in too low an abundance to reasonably achieve a sample for analysis. The yellow shaded regions in each panel represent previously published cell content ranges: C - Casey et al.<sup>20</sup>; N-Bertilsson et al.<sup>9</sup> for *Prochlorococcus* and *Synechococcus*, and Ho et al.<sup>26</sup> for picoeukaryotes; P-Bertilsson et al.<sup>9</sup> for *Prochlorococcus* and *Synechococcus*, and Ho et al.<sup>26</sup> and Whitney and Lomas<sup>27,28</sup> for picoeukaryotes.

regions (Fig. 2 and Supplementary Table 2), showing no discernable regional control on cell nutrient content. Elemental concentrations of C from field populations generally agreed well with the range of values previously summarized<sup>20</sup>; 2–28 fmol C cell<sup>-1</sup>, 4–77 fmol C cell<sup>-1</sup>, and 4–795 fmol C cell<sup>-1</sup> for *Prochlorococcus*, *Synechococcus*, and picoeukaryotes, respectively. Although in some instances (e.g., ETNP) measured values for *Prochlorococcus* and *Synechococcus* exceeded the published range, but by no more than a factor of two. Published data for cellular N and P content are more scarce, however, values determined in this

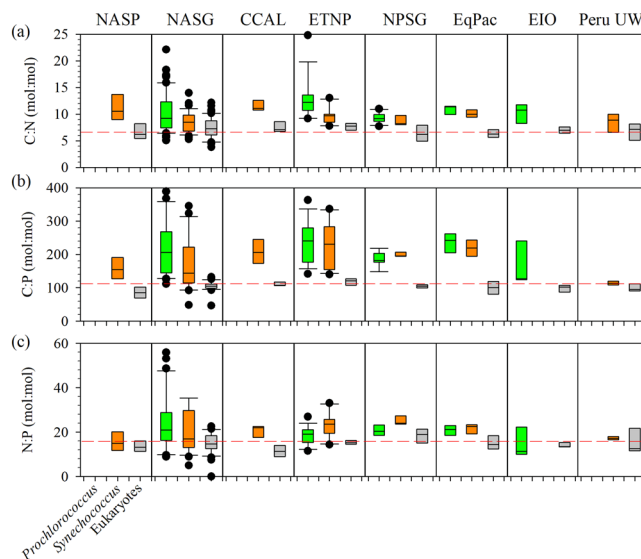


**Fig. 3** Elemental stoichiometric ratios for each phytoplankton population in each ocean region. Box-Whisker plots of (a) C:N (mol:mol), (b) C:P (mol:mol), and (c) N:P (mol:mol) ratios for (L to R within a region) *Prochlorococcus*, *Synechococcus*, and eukaryotes in each of the eight ocean regions as noted at the top of a and defined in Fig. 1. The box defines the 25% and 75% quartiles, the line through the box is the mean, the error bars represent the 5% and 95% distribution limits, and black circles represent data points outside this range. Where there are no box/whisker plots, there are no available data.

study agree within a factor of two of published data from culture studies (Fig. 2).

**Stoichiometric ratios.** We explored elemental stoichiometric ratios between different taxonomic populations to determine whether previously observed taxonomic differences in the North Atlantic<sup>18,21</sup> are observed in other regions. *Prochlorococcus* and *Synechococcus* populations consistently were found to have mean elemental C:N ( $11 \pm 4$ ;  $9 \pm 2$ , respectively), C:P ( $228 \pm 77$ ;  $188 \pm 68$ , respectively) and N:P ( $22 \pm 9$ ;  $21 \pm 7$ , respectively) ratios that were 0.5- to twofold higher than the canonical Redfield Ratio<sup>3,4</sup>. In contrast, the C:N ( $7 \pm 2$ ), C:P ( $103 \pm 15$ ), and N:P ( $15 \pm 4$ ) ratios of co-occurring eukaryotes were both less variable and much closer to the Redfield ratio (Fig. 3 and Supplementary Table 3; Taxa x Region ANOVA, all pairwise comparisons  $P$  value  $< 0.01$ ). There were exceptions, such as the nutrient-rich Peru upwelling (Peru UW) where *Synechococcus* C:P ratios were similar to the C:P ratio of co-occurring eukaryotes, and the subtropical N. Atlantic (NASP), where *Synechococcus* had a median C:P ratio that was twice that of co-occurring eukaryotes, but was still low compared to other regions in the data set. In these two nutrient-rich systems, *Prochlorococcus* was not present in sufficient numbers to sort for a meaningful elemental analysis, so we cannot assess if this is a general cyanobacterial response to nutrient-rich conditions. The Pacific equatorial upwelling, which is intermediate in near-surface nutrient concentrations and where *Prochlorococcus* populations were sorted, did not elicit a reduced C:P ratio in either cyanobacterial population. Significant differences in stoichiometric ratios between *Prochlorococcus* and *Synechococcus* were only observed in the NASG. Comparisons within a taxonomic group between different regions showed no significant differences, although median values often varied by 25–50% between regions.

Why are elemental stoichiometric ratios of cyanobacteria, in nutrient-depleted ocean regions, consistently higher than the

canonical Redfield ratio and that of co-occurring eukaryotes? To explore if these differences are owing to elevated C content or reduced N and P contents, we compare our data to published elemental quota data (Supplementary Figure 2). Given the unknown, but quite likely variable, physiological state of the field samples in this study, published data were taken from both culture and natural population data, and which included both nutrient-replete and nutrient-deplete growth conditions. The literature values are presented with their complete range to better reflect this wide range of environmental variables and growth conditions. *Prochlorococcus* ( $80 \pm 27 \text{ fmol } \mu\text{m}^{-3}$ ) and *Synechococcus* ( $46 \pm 30 \text{ fmol } \mu\text{m}^{-3}$ ) were found to have mean cell C quotas outside the range of published values, 15–40  $\text{fmol } \mu\text{m}^{-3}$  (22–24). The sorted eukaryotic populations, unlike the picocyanobacteria populations, are a diverse mix of taxa grouped by similarity in size. Small eukaryotes, deemed similar in size to those sorted in this study, have a C quota range of 9–18  $\text{fmol } \mu\text{m}^{-3}$  (25,26), a range that is higher than the mean cell quota observed in this data set,  $5 \pm 2 \text{ fmol } \mu\text{m}^{-3}$ . Similar patterns are seen for N and P quotas. Mean N quotas for *Prochlorococcus* ( $8 \pm 3 \text{ fmol } \mu\text{m}^{-3}$ ) and *Synechococcus* ( $5 \pm 3 \text{ fmol } \mu\text{m}^{-3}$ ) is greater than the range found in the literature, 1.4–4.0  $\text{fmol } \mu\text{m}^{-3}$  (9,24), whereas the mean N quota of eukaryotes ( $0.6 \pm 0.4 \text{ fmol } \mu\text{m}^{-3}$ ) was within the estimated published range (0.3–2  $\text{fmol } \mu\text{m}^{-3}$ , 9,26). Mean P quotas for *Prochlorococcus* ( $0.2 \pm 0.1 \text{ fmol } \mu\text{m}^{-3}$ ) and *Synechococcus* ( $0.1 \pm 0.1 \text{ fmol } \mu\text{m}^{-3}$ ) are more similar to the range found in the literature, 0.03–0.12  $\text{fmol } \mu\text{m}^{-3}$  (9,24), whereas the mean P quota of eukaryotes ( $0.04 \pm 0.03 \text{ fmol } \mu\text{m}^{-3}$ ) was within the estimated published range (0.02–0.25  $\text{fmol } \mu\text{m}^{-3}$ , 9,26–28). This analysis suggests a fundamental difference between natural populations of cyanobacteria and eukaryotes of similar size, with cyanobacteria from this study consistently showing greater cell C quotas than previously published data, whereas eukaryotes consistently show lower cell C quotas. Although the physiological mechanisms cannot be confirmed with the data in hand, our data are consistent with prior research that found significantly greater biomass-specific C fixation rates in cyanobacteria than co-occurring eukaryotes<sup>29</sup>, which may lead to the observed increases in C quotas.

**Environmental correlates.** We explore environmental controls to explain the variability in cell contents and stoichiometric ratios (Table 1 and Supplementary Figures 3–7). First, we use depth as a proxy for the light environment to which the cells were exposed. Across the entire data set, C content in *Prochlorococcus* increased significantly (Model 1 regression,  $P < 0.05$ ) with depth, while P content in *Prochlorococcus* exhibited a marginally significant increase with depth. A similar pattern for C has been reported previously in data from the subtropical North Atlantic<sup>20</sup> and cultures<sup>30</sup>. The only other significant relationship observed with depth was for *Synechococcus* N content. This is likely due to photoacclimation and increases in cellular pigments containing N<sup>31,32</sup>. Chlorophyll has 4 N atoms in its structure and thus increases in chlorophyll pigment would increase cellular nitrogen content, although it would increase C content to a greater degree (chlorophyll C:N ratio 13.5:1). It is more likely that an increase with depth in N-rich phycobilisomes<sup>33</sup> led to the increase in *Synechococcus* cellular N quota without an increase in C (Table 1 and Supplementary Figures 3 and 6). This explanation also is consistent with the lack of relationship between N quota and depth for *Prochlorococcus*, as this genus does not use phycobilisomes, but rather a much more N efficient light-harvesting system<sup>34,35</sup>.

Temperature is known to regulate a wide range of physiological and cellular processes<sup>36,37</sup>. Across the entire data set, *Prochlorococcus*

showed a significant negative relationship between cellular C content and temperature, while *Synechococcus* showed a significant negative relationship between cellular P content and temperature (Table 1 and Supplementary Figure 4). The observations for *Synechococcus* and P content are consistent with lab studies<sup>38,39</sup>, although the observations for *Prochlorococcus* are not. In general, however, these trends in cyanobacteria populations are consistent with the notion that higher temperatures are associated with ocean gyres, which are more likely to be nutrient-deplete leading to a range of physiological adjustments including higher relative rates of release for newly fixed C<sup>40</sup> and reductions in cellular P-containing metabolites<sup>41</sup>. In contrast, for the Eukaryotes, there is a marginally significant (Table 1) positive relationship between both cellular C and P and temperature. Further, the trend in the data presents itself as an “envelope” setting a maximum upper limit rather than a predictive relationship between variables (Supplementary Figure 4). Although physiological versus taxonomic differences cannot be resolved for this “population” as it contains an unknown diversity of eukaryotes of similar size, the observation of increasing cell contents is consistent with phytoplankton temperature-dependent growth response envelopes<sup>42</sup> and the observed differential responses to an increasing temperature between cultured strains<sup>36</sup>.

Nearly half of the cellular stoichiometric ratios showed a significant, or marginally significant, relationship with temperature (Table 1 and Supplementary Figure 7). C:P ratios, but not N:P ratios, for *Synechococcus* and eukaryotes were positively related with temperature; an observation consistent with recent research<sup>43,44</sup>. In this study, for *Synechococcus* the increase in C:P ratio is the result of reduced P contents with temperature, consistent with the temperature-dependent physiology hypothesis<sup>45</sup>. However, for the eukaryotes, the response was more complicated, due to the observation that both cellular C and P increased with temperature (Supplementary Figure 4), although the greater temperature sensitivity of C, relative to P, led to the significant increase in C:P. The relationships between C:N:P and temperature are more complex and species-specific than presented by Yvon-Durocher<sup>44</sup>.

Absolute nutrient concentrations and nutrient ratios are well known to regulate cellular particulate stoichiometric ratios in a wide range of species<sup>46</sup>. Here, we examined nutrient ratios in two formats; the ratio of ambient residual nutrient stocks at the depth from which samples were collected, and the ratio of vertical nutrient fluxes across the nutricline, which in most cases was at the base of the euphotic zone (see Baer et al.<sup>18,47</sup> for more information on this approach). The nutrient flux ratio is more impactful to phytoplankton in the deepest samples as this represents the ratio supplied by vertical mixing and upwelling<sup>48</sup>. No cell contents or stoichiometric ratios were significantly correlated with measured ambient residual nitrate:phosphate nutrient ratios. Although this result is in contrast to recent publications<sup>2</sup>, it is not unexpected given that surface concentration ratios are not expected to be representative of phytoplankton uptake ratios and further are skewed by analytical uncertainty at low ambient nutrient concentrations which can impact ratio calculations. In contrast, *Prochlorococcus* and *Synechococcus* both showed cell contents that were negatively correlated with increasing ratios of vertical nitrate:phosphate fluxes (Supplementary Figure 5). This relationship appeared more as a “threshold”, where above nitrate:phosphate flux ratios of ~24:1 cell contents of C and P attained a minimum and remained at this level while at flux ratio values less than ~24:1, cell contents spanned the entire observed range. This type of inverse rectilinear response is very similar to the response seen in critical nutrient ratio experiments<sup>11,49</sup> that demonstrate the nitrate:phosphate availability ratio where cells transition from N to P limitation. While eukaryote cell contents



**Table 1 Correlations between measured environmental variables and cellular contents and stoichiometric ratios for each taxonomic group.**

Taxa	Parameter	Depth (irradiance proxy)			Temperature			NO <sub>3</sub> :PO <sub>4</sub> flux		
		R	P value	N	R	P value	N	R	P value	N
<i>Prochlorococcus</i>	C	<b>0.41</b>	<b>&lt;0.01</b>	<b>84</b>	<b>-0.29</b>	<b>&lt;0.01</b>	<b>74</b>	<b>-0.31</b>	<b>&lt;0.01</b>	<b>70</b>
	N	0.15	0.17	81	0.04	0.77	67	<b>-0.27</b>	<b>0.03</b>	<b>67</b>
	P	0.21	0.08	72	-0.13	0.28	66	<b>-0.26</b>	<b>0.04</b>	<b>65</b>
	C:N	<b>0.29</b>	<b>&lt;0.01</b>	<b>85</b>	<b>-0.46</b>	<b>0.01</b>	<b>73</b>	-0.22	0.07	73
	C:P	0.10	0.44	62	-0.08	0.58	56	<b>0.35</b>	<b>&lt;0.01</b>	<b>55</b>
	N:P	-0.18	0.17	59	0.25	0.08	53	<b>0.69</b>	<b>&lt;0.01</b>	<b>52</b>
<i>Synechococcus</i>	C	0.04	0.72	70	-0.21	0.13	56	<b>-0.32</b>	<b>0.02</b>	<b>56</b>
	N	<b>0.28</b>	<b>0.02</b>	<b>64</b>	-0.20	0.16	50	-0.03	0.82	51
	P	0.11	0.41	60	<b>-0.35</b>	<b>0.02</b>	<b>42</b>	<b>-0.38</b>	<b>0.02</b>	<b>41</b>
	C:N	-0.09	0.49	60	<b>-0.29</b>	<b>0.05</b>	<b>50</b>	0.01	0.97	51
	C:P	-0.19	0.19	49	0.28	0.07	41	<b>0.32</b>	<b>0.05</b>	<b>40</b>
	N:P	-0.19	0.21	47	0.27	0.12	35	0.33	0.06	34
Eukaryotes	C	0.06	0.60	87	0.22	0.06	73	-0.14	0.22	76
	N	0.11	0.34	84	0.15	0.23	71	-0.11	0.34	71
	P	-0.01	0.95	74	0.21	0.12	59	0.10	0.46	58
	C:N	-0.05	0.67	75	0.01	0.91	70	<b>0.31</b>	<b>&lt;0.01</b>	<b>71</b>
	<b>C:P</b>	<b>-0.29</b>	<b>0.04</b>	<b>52</b>	<b>0.43</b>	<b>&lt;0.01</b>	<b>49</b>	<b>0.37</b>	<b>&lt;0.01</b>	<b>49</b>
	N:P	0.13	0.36	51	0.28	0.07	45	<b>0.35</b>	<b>0.02</b>	<b>45</b>

Correlations were tested using the Pearson Product Moment Correlation test for each taxa/element content pair and selected environmental variables. The strength of correlation (R), the significance of correlation (P value), and a number of discrete data points in the correlation (N) are shown for each correlation. Significant (P value <0.05) correlations are shown in bold font, marginally significant (P value >0.05<0.10) correlations are shown in italics.

were not significantly correlated with nitrate:phosphate flux ratios and cell contents did not demonstrate the rectilinear response seen in the cyanobacteria lineages, there was an upper limit to observed cell content values, which did decrease with increasing nitrate:phosphate flux ratios.

Of the environmental variables examined, it was the vertical nitrate:phosphate flux ratios that most consistently (eight out of nine relationships were significant or marginally so) explained variance in elemental stoichiometric ratios. As anticipated, vertical nitrate:phosphate flux ratios were positively correlated with C:P and N:P ratios in all taxonomic groups, although the magnitude of the response varied (Fig. 4 and Table 1). The cyanobacterial populations displayed a greater increase in C:P and N:P ratios than the eukaryotes, an observation consistent with previous work by this group of researchers<sup>5</sup>. The increases in C:P and N:P ratios are driven primarily by decreases in cellular P contents (Supplementary Figure 5), as expected, in response to increasing P-stress. The damped response of C:P and N:P ratios in eukaryotes could arise from nutrient co-limitations<sup>50</sup> that limit their plasticity with regard to P. For example, it has been shown that eukaryotes, in response to extreme P-stress replace P-containing lipids with N-containing lipids<sup>41</sup>. In the nutrient-deplete regions, where most of these samples were collected, N concentrations are also exceedingly low and thus may limit the ability of eukaryotes to modulate their P content. In contrast, the cyanobacteria genera readily swap P-containing lipids for sulfur-containing lipids. Perhaps a more likely explanation is that eukaryotes are supplementing their autotrophic nutrition with mixotrophy<sup>51</sup>. Pigmented eukaryotes of the size that were sorted in this study have been shown to dominate bacterivory in the ocean and can obtain up to 25% of the nutrient demand from this mixotrophic nutritional mode<sup>52</sup>.

C:N ratios in *Prochlorococcus*, but not *Synechococcus* were negatively related to vertical nitrate:phosphate flux ratios, but this is largely driven by high cellular C:N values when vertical nitrate:phosphate flux ratios decreased below the Redfield Ratio of 16:1. This suggests that below a flux ratio of 16:1,

conditions of increasing relative N-stress, *Prochlorococcus* continues to accumulate cellular C via photosynthesis<sup>29</sup> although there are questions on whether that newly fixed C is retained<sup>40,53</sup>. In contrast, the eukaryotic C:N ratios were positively correlated with nitrate:phosphate flux ratios, driven by a greater relative reduction in N content than C content in response to increasing vertical nitrate:phosphate flux ratios. The observation that within taxonomic group variance in stoichiometric ratios can be explained by the relative input of potentially limiting macronutrients suggests that the optimal allocation phytoplankton model proposed by Sharoni and Halevy may have more than one “solution” or is not always the best model to explain bulk particulate organic matter stoichiometric ratios<sup>6</sup>.

**Predicting particulate organic matter ratios.** Due to the analytical challenges associated with generating these data, directly assessing the relationships between phytoplankton stoichiometry and bulk POM at broader scales is difficult. To assess if taxonomic variability in stoichiometric ratios was an important control on bulk POM ratios<sup>6–8</sup>, we evaluated two models for the prediction of bulk POM stoichiometric ratios. First, was the “optimal-growth” phytoplankton model that only takes into consideration the relative abundance of taxonomic groups and a mean stoichiometric ratio for each group<sup>6</sup>. In this model, the relative C biomass abundance of taxonomic groups was scaled by a constant mean group-specific stoichiometric ratio compiled from the published literature (Supplementary Table 4). The predicted POM stoichiometry is the weighted mean of the relative abundance of phytoplankton taxa multiplied by these ratios. Because the model assumes that the resident phytoplankton are growing at an invariant “optimum” stoichiometric ratio, then any relationships between observed bulk POM ratios and this model output results from changes in phytoplankton community composition. Second, we assessed an “acclimation” model that considers the relative abundance of taxonomic groups, identical to the optimum-growth model, but calculates a sample-specific

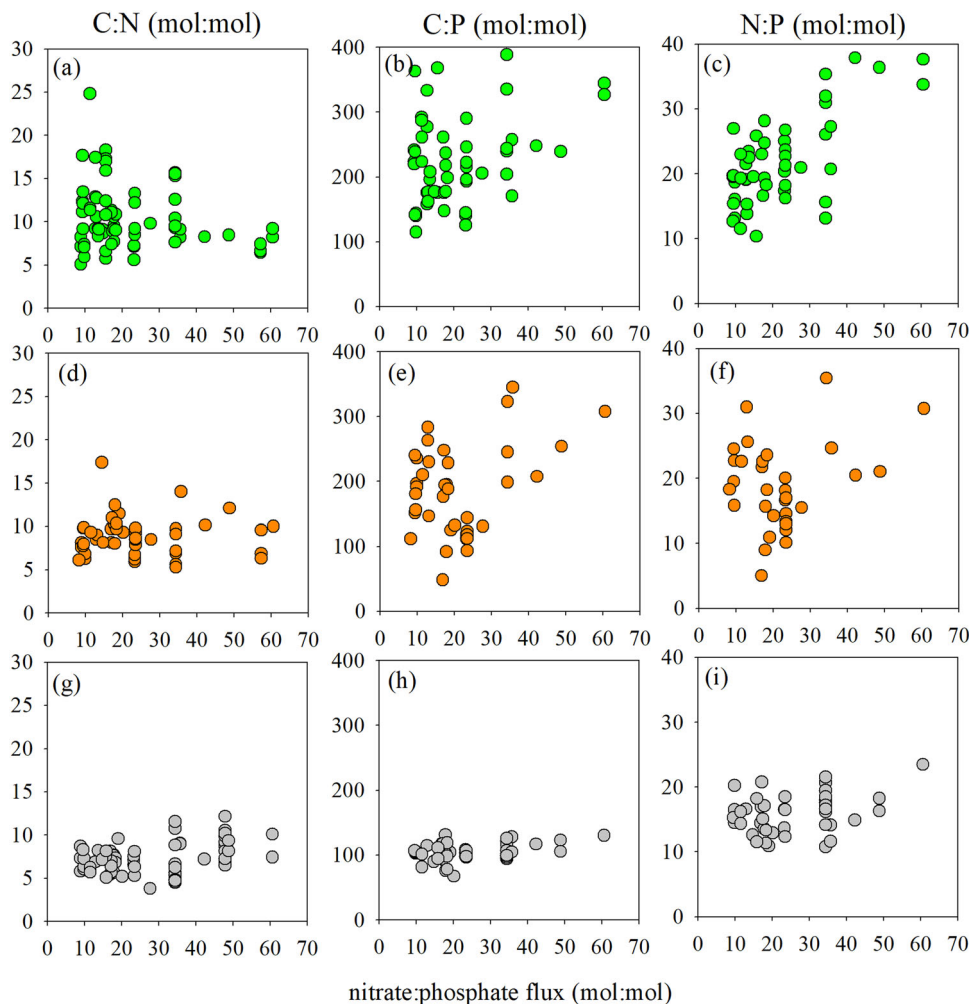


**Fig. 4** Relationship of cellular stoichiometric ratios to vertical nitrate:phosphate fluxes across the nutricline. (a–c) *Prochlorococcus*; (d–f) *Synechococcus*; and (g–i) Eukaryote populations and C:N (a, d, g), C:P (b, e, h), and N:P (c, f, i) ratios (mol:mol).

stoichiometric ratio rather than using the literature-based optimum value. A multiple linear regression model was used to calculate the group-specific stoichiometric ratios based upon the temperature, depth, and vertical nitrate:phosphate flux ratios (Supplementary Table 5), at each station/depth, which was then scaled to the relative C biomass of each group in this model. We used both models to predict bulk POM stoichiometric ratios, which this research team directly measured along transects from 19°N to 55°N in the western N. Atlantic Ocean and from 19°N to 3°S in the central Tropical/Equatorial Pacific (Fig. 5 and Supplementary Figures 8–9).

Both models provided a reasonable representation of the bulk particulate stoichiometric ratios over portions of both transects (Fig. 5 and Supplementary Figures 8–9). This suggests that to a first-order phytoplankton community composition is an important driver of bulk POM stoichiometry ratios, otherwise, model output and observations would not agree as often as was seen. However, our data set does not have a great enough “dynamic range” in the phytoplankton community composition, most samples were from oligotrophic regions and we did not quantify large phytoplankton in the nutrient-rich regions, to find a significant predictive correlation between phytoplankton communities and bulk POM ratios.

C:N ratios varied little along either transect with no significant differences between observations and model outputs (Supplementary Figure 8). This result for C:N ratios are perhaps expected

as prior studies have shown similarly narrow ranges of bulk POM C:N ratios<sup>21</sup>. Furthermore, different picoplankton populations from the western North Atlantic, flow cytometrically sorted as in this study, are only marginally different from each other in terms of the C:N ratios<sup>21</sup>. Bulk POM N:P ratios showed expected trends, with bulk POM N:P ratios along the N. Atlantic transect increasing from ~10:1 in the north to ~20:1 in the south, whereas along with the tropical Pacific transect values remained roughly constant at ~20:1 (Supplementary Figure 9). Significant differences between model outputs and bulk POM N:P ratios were few and only occurred at the transition from the subpolar gyre to the subtropical gyre (~40°N) along the N. Atlantic transect. Although differences were not significant for most stations, mean N:P ratios from the optimal-growth model were consistently greater than N:P values from the acclimation model as the fixed stoichiometric N:P ratios in the optimum-growth model were not fully compensated by the shift from a population dominated by cyanobacteria to one dominated by eukaryotes. This result supports the hypothesis that phytoplankton community structure and acclimation to local conditions interact to modulate stoichiometric ratios in these populations. Changes in stoichiometric C:P ratios more clearly highlighted the potential interplay between phytoplankton community composition and acclimation to the local environment. Along the N. Atlantic transect, bulk POM stoichiometric ratios significantly increased (station by station comparison, Student’s *t* test,  $P < 0.05$ ) once south of ~30°N, an

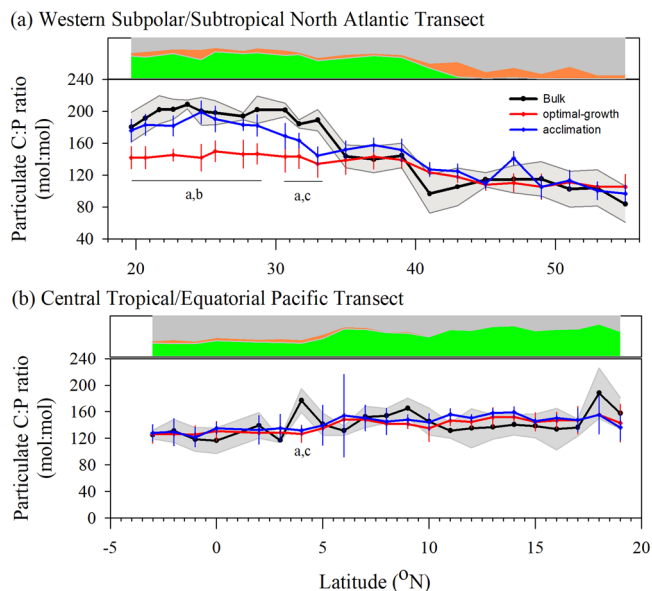


**Fig. 5 Measured and modeled euphotic zone particulate carbon-to-phosphorus stoichiometric ratios.** Euphotic zone averaged particulate organic carbon-to-phosphorus (C:P) stoichiometric ratios along (a) a transect in the western North Atlantic Ocean and (b) a transect in the central Tropical/Equatorial Pacific. The black line is the euphotic zone (0–100 m) average ratio of bulk POM measurements, and the gray shading is the 95% confidence interval around the euphotic zone average ratio. The red line is the optimal-growth phytoplankton model estimate of particulate C:P ratio, and the blue line is the acclimation model estimate of particulate C:P ratio. For both models, the error bars at each station represent the 95% confidence interval range. The western North Atlantic transect was comprised of two cruises, both in August/September, with the northern half (31°N–55°N) conducted in 2013 (Cruise AE1319), and the southern half (19°N–33°N) conducted 2014 (BVal 47). The central Tropical/Equatorial Pacific transect was a single cruise (NH1418). Significant differences between models and observations at each station are represented in the following manner: ‘a’-observations are significantly different from the predictions of the optimal-growth model; ‘b’-predictions from the optimal-growth model are significantly different from the predictions of the acclimation model; and ‘c’-observations are significantly different from the predictions of the acclimation model. Above each panel is a stacked area plot of the relative contribution of cyanobacteria *Prochlorococcus* (green fill), *Synechococcus* (orange fill), and eukaryotes (gray fill) to total measured autotrophic C along the transect.

observation previously noted in this region<sup>5</sup> and consistent with the hypothesis that this region is P-stressed<sup>54–56</sup>. The stoichiometric ratios from the optimal-growth model increased only slightly, owing to the increase in relative biomass of *Prochlorococcus*, and were significantly lower than the bulk POM stoichiometric ratios. In contrast, the stoichiometric ratios from the acclimation model tracked bulk POM in this region and were not significantly different, supporting the contention of nutrient control of stoichiometric ratios<sup>2</sup>. Furthermore, this increase in bulk POM and acclimation model stoichiometric ratios is consistent with the increase in the vertical nitrate:phosphate flux ratio along this transect<sup>18</sup>. The transect in the tropical Pacific, however, did not show any significant differences between either model and the observed bulk POM stoichiometric ratios, despite similarly low nutrient concentrations over much of the transect. A possible explanation for this is the suggestion that the Pacific in this region could be N-stressed<sup>57</sup>, rather than P-stressed. At least for *Synechococcus*, N-stress has been shown to have no meaningful impact on any of the stoichiometric ratios, unlike P-stress, which

leads to significant changes in the N:P and C:P ratios<sup>58</sup>. If the nutrient-stress response of stoichiometric ratios seen in *Synechococcus* is mirrored in *Prochlorococcus*, the dominance of *Prochlorococcus* in the autotrophic community could definitely explain the limited variability in bulk stoichiometric ratios and the lack of difference between the optimal-growth and acclimation models.

These models show that controls on bulk POM stoichiometry are more complicated than recently concluded<sup>6</sup>. Both phytoplankton biodiversity and acclimation to the local environment are important controlling factors of bulk POM stoichiometry and these controls differ between ocean regions. Sharoni and Halevy recently concluded that phytoplankton are well-adapted to their ambient nutrient environment in all ocean regions modeled, however, our data show that it is the ratio of nitrate:phosphate inputs that drive cellular acclimation responses, a conclusion also reached in chemostat culture studies<sup>10</sup>. We conclude that biogeochemical models should include both phytoplankton biodiversity and cellular acclimation to vertical nutrient flux ratio controls in predictions of particulate stoichiometry and ocean biogeochemistry.

### Concluding remarks

Our observations of cellular macronutrient, C, N, and P, content in populations of marine cyanobacteria and small eukaryotes from a wide range of ocean regions are generally consistent with data from cultured strains but present a significant advance as they are direct measures of field populations. The resulting stoichiometric ratios confirmed prior observations of cyanobacteria having consistently and significantly higher ratios than co-occurring eukaryotes, with one notable exception. *Synechococcus* populations in the nutrient-enriched Peru upwelling region displayed C:P and N:P ratios that were similar to that of eukaryotes. This observation supports our conclusion that while baseline stoichiometric ratios are taxonomically linked; cellular ratios are not “fixed” but rather are modulated in response to the local environment, in particular nutrient inputs. Whether this modulation arises purely from physiological plasticity or from changes in a dominant genotype, particularly in cyanobacteria<sup>59</sup>, remains to be completely resolved.

Ambient light levels (using collection depth as a proxy) and temperature were not found to be consistent environmental drivers and only a subset of element/taxa combinations were significantly related to these environmental variables. In stark contrast, the ratio of nitrate:phosphate mixing into the euphotic zone across the nutricline correlated with nearly all element/taxa cell contents and stoichiometric ratios. This highlights that despite recent assertions, evidence from direct observations shows that physiological acclimation to local nutrient supply is important to understand variance in observed cellular macronutrient contents and stoichiometric ratios and that the degree of acclimation may differ between prokaryotic and eukaryotic taxa. Further, predictions of particulate C:P ratios compared more favorably when this environmental acclimation was considered.

### Methods

**Phytoplankton sample collection and preparation.** Samples were collected from cruises in several major ocean basins (Supplementary Table 1). Samples for taxon-specific elemental content were collected using 12 L Niskin bottles, along with electronic CTD sensor data (temperature, salinity, in vivo chlorophyll fluorescence, dissolved oxygen), usually from two depths at each station; one within the upper mixed layer (10–20 m) and one near the deep chlorophyll maximum. Owing to the timing of the cruises, samples were collected from a seasonal window limited to summer and early fall. Samples were prepared for sorting by concentrating cells from the ambient sample under darkened conditions using a Menteq High Volume Cell Trap (0.2 μm pore size)<sup>60</sup>, and then flushed from the Cell Trap using 0.2 μm filtered seawater and a luer lock syringe; roughly 3–4 L of ambient seawater was concentrated down to ~5 mls. Samples were either gravity filtered through the Cell Trap directly from the Niskin bottle or pushed through the cell trap



using a peristaltic pump at  $<50 \text{ ml min}^{-1}$ . Samples were then kept cool at  $4^\circ\text{C}$  if they were going to be sorted live and immediately after collection or fixed with freshly filtered paraformaldehyde (0.5% v/v final concentration) if they were going to be stored for later sorting. Samples were allowed to fix at  $4^\circ\text{C}$  for 1–2 h and then flash-frozen in liquid nitrogen and then moved to  $-80^\circ\text{C}$  for longer-term storage.

**Cell sorting and elemental analysis.** The cell counting and sorting protocols followed that of Baer et al.<sup>18</sup> as summarized here. Cell counts and sorts were performed on either a Becton Dickinson Influx or FACSJazz flow cytometer, each utilizing a 200 mW 488 nm laser, with detectors for forward scatter, side scatter, 692 nm, and 530 nm, and operated with 8 g NaCl  $\text{kg}^{-1}$  solution for sheath fluid, which was filtered inline using a 0.22  $\mu\text{m}$  Millipore Sterivex™ filter. Instrument alignment was performed with 3.0  $\mu\text{m}$  6-peak rainbow beads, while roughly hourly checks on forward scatter response were performed with 0.53  $\mu\text{m}$  Nile Red beads (Spherotech). *Prochlorococcus* populations were discriminated based on forward scatter and red fluorescence, and a gate in orange (530 nm) discriminated for *Synechococcus*. Eukaryotes were all larger autofluorescing cells that did not fit the cyanobacterial gating scheme. For sorting, sort control software was set to “1.0 drop pure” sort mode. In excess of 17 million, 8 million, and 500,000 cells for *Prochlorococcus*, *Synechococcus*, and eukaryotes were sorted for chemical analysis, respectively. Not all phytoplankton groups were sufficiently abundant at each station/depth for practical sorting and subsequent analysis. Post-sort purity tests were run with subsamples of each sorted population; sort purity always exceeded 94%. Sorted populations were collected in polystyrene Falcon tubes (BD Biosciences Inc.) and subsequently filtered on pre-combusted (450°C for 4 h) GF-75 filters (Ahlstrom; nominal pore size = 0.3  $\mu\text{m}$ ). To ensure complete capture of all of the cells, the Falcon tubes were rinsed multiple times with 0.2  $\mu\text{m}$  filtered sheath fluid. Filter and sheath fluid blanks were produced each day samples were sorted for subsequent subtraction from the mass of each unknown sample. Following filtration, filters were placed in acid-washed cryovials and frozen ( $-20^\circ\text{C}$ ) until analysis as described below. Average cellular elemental content was determined by dividing the elemental content of the sample by the number of sorted cells as determined in a direct post-sort count analysis of the sorted sample. Data are publicly accessible<sup>61</sup>.

**Dissolved nutrients and fluxes.** Nutrient samples were collected after filtration through 0.8  $\mu\text{m}$  polycarbonate filters. Inorganic nutrient concentrations were analyzed using standard protocols and calibrations on an air-segmented autoanalyzer<sup>62–64</sup>;  $\text{NO}_3^-$  detection limit = 30  $\text{nmol N kg}^{-1}$ , and  $\text{PO}_4^{3-}$  detection limit = 50  $\text{nmol kg}^{-1}$ . On all cruises, except for NH1410, SO243, RR1604, SPOTS, and Newport Pier, soluble reactive P (SRP) concentrations were also measured via the magnesium-induced co-precipitation method<sup>65,66</sup> with modifications as per Lomas et al.<sup>55</sup>; detection limit = 1  $\text{nmol P kg}^{-1}$ . P sample concentrations were calculated against a potassium monobasic phosphate standard prepared in P-free seawater<sup>55</sup>, and a certified phosphate standard (Ocean Scientific International Ltd. Phosphate Nutrient Standard Solution) was used for quality control with each analytical run.

Diapycnal nitrate:phosphate flux ratios were calculated directly from the slope of nutrient concentration profiles under the assumption that the vertical diffusivity coefficients would apply equally to both nutrients, and thus a value for diffusivity was not needed in the calculation. The slope of the nutrient profile was calculated across the nutricline, defined as the depth where nutrient concentrations exceeded the analytical limit of quantitation for each nutrient, which varied from region to region depending upon local conditions.

**Particulate nutrients.** Particulate organic P (POP) was analyzed using the ash-hydrolysis method<sup>55</sup>, with oxidation efficiency and standard recovery tested with each sample run using an ATP standard solution and a certified phosphate standard (OSIL Phosphate Nutrient Standard Solution). Method precision is 1–2% at 5  $\text{nmol kg}^{-1}$ . Samples for POC and PON were acid fumed in a desiccator over concentrated HCl prior to analysis. After acid fuming, POC and PON were determined on a Costech 4010 elemental analyzer or a Control Equipment 440 elemental analyzer, depending on the samples. L-glutamic acid (USGS40) was used for standard curve generation and as a check standard (tolerance of  $<0.1 \mu\text{g}$ ) approximately every ten samples and at the end of every instrument run. Empty tin capsules (Costech Analytical Technologies) were cleaned with acetone and dried and run as instrument blanks.

**Elemental stoichiometry models.** The elemental cell quota data determined in this study were used in mathematical models to estimate calculated phytoplankton community stoichiometric ratios in comparison with concurrent measurements of bulk particulate organic matter ratios (Supplementary Data 1). Full details of model calculations are provided in the Supplemental Information text. In brief, two models were used, one was an optimal-growth model using cellular stoichiometric data from culture experiments in the published literature (Supplementary Table 4) where growth rates were not limited. The other model was an acclimation model where elemental cell quota data collected in this study were related to ambient environmental variables (temperature, depth, and nitrate:phosphate vertical flux)

with a least-squares multiple linear regression model and the resulting equations used to estimate stoichiometric ratios across the broader range of stations/depths (Supplementary Table 5). For both models, the estimates of cellular stoichiometric ratios were then scaled to the relative abundance of *Prochlorococcus*, *Synechococcus*, and eukaryotes.

**Statistical analyses.** All statistical analyses were done in SigmaStat Version 3.5 (Systat Software, San Jose, CA).

## Data availability

Data can be found under the corresponding author’s name at the Biological-Chemical Oceanography Data Management Office, Project title “Biological Control on the Ocean C:N:P ratio” (<http://bco-dmo.org/project/2178>). Phytoplankton cell quota data from flow cytometrically sorted natural populations have the following citation information: “Direct measure of phytoplankton cell quotas from field populations sampled from multiple cruises between 2010 and 2016”, 2021-06-03, <https://doi.org/10.26008/1912/bco-dmo.849153.1>. Bulk data used in the stoichiometric model portion of the manuscript can be found here: Lomas, M. W., Martiny, A. (2020) Depth profile data from R/V New Horizons NH1418 in the tropical Pacific from Sept-Oct. 2014. Biological and Chemical Oceanography Data Management Office (BCO-DMO). (Version 1) Version Date 2020-11-19, <https://doi.org/10.26008/1912/bco-dmo.829895.1>, and Lomas, M. W., Martiny, A. (2020) Depth profile data from R/V Atlantic Explorer AE1319 in the NW Atlantic from Aug-Sept. 2013. Biological and Chemical Oceanography Data Management Office (BCO-DMO). (Version 1) Version Date 2020-11-18, <https://doi.org/10.26008/1912/bco-dmo.829797.1>.

Received: 4 January 2021; Accepted: 23 June 2021;

Published online: 14 July 2021

## References

- Kwiatkowski, L., Aumont, O., Bopp, L. & Ciais, P. The impact of variable phytoplankton stoichiometry on projections of primary production, food quality and carbon uptake in the global ocean. *Glob. Biogeochem. Cycle* **32**, 516–528 (2018).
- Moreno, A. R. & Martiny, A. C. Ecological stoichiometry of ocean plankton. *Annu. Rev. Marine Sci.* **10**, 43–69 (2018).
- Redfield, A. In *James Johnstone Memorial Volume* 176–192 (Liverpool University Press, 1934).
- Redfield, A. The biological control of chemical factors in the environment. *Am. Sci.* **46**, 205–221 (1958).
- Martiny, A. C. et al. Strong latitudinal patterns in the elemental ratios of marine plankton and organic matter. *Nat. Geosci.* **6**, 279–283 (2013).
- Sharoni, S. & Halevy, I. Nutrient ratios in marine particulate organic matter are predicted by the population structure of well-adapted phytoplankton. *Sci. Adv.* **6**, eaaw9371 (2020).
- Arrigo, K. et al. Phytoplankton community structure and the drawdown of nutrients and  $\text{CO}_2$  in the Southern Ocean. *Science* **283**, 35–367 (1999).
- Weber, T. & Deutsch, C. Ocean nutrient ratios governed by plankton biogeography. *Nature* **467**, 550–554 (2010).
- Bertilsson, S., Berglund, O., Karl, D. M. & Chisholm, S. W. Elemental composition of marine *Prochlorococcus* and *Synechococcus*: implications for the ecological stoichiometry of the sea. *Limnol. Oceanogr.* **48**, 1721–1731 (2003).
- Leonardos, N. & Geider, R. J. Responses of elemental and biochemical composition of *Chaetoceros muelleri* to growth under varying light, nitrate:phosphate supply ratios and their influence on the critical N:P. *Limnol. Oceanogr.* **49**, 2105–2114 (2004).
- Rhee, G. Effect of N:P atomic ratios and nitrate limitation on algal growth, cell composition, and nitrate uptake. *Limnol. Oceanogr.* **23**, 10–25 (1978).
- Galbraith, E. & Martiny, A. C. A simple nutrient-dependence mechanism for predicting the stoichiometry of marine ecosystems. *Proc. Acad. Nat. Sci. Phila.* **112**, 8199–8204 (2015).
- Longhurst, A. R. *Ecological Geography of the Sea*. (Academic, 1998).
- Frigstad, H. et al. Seasonal variation in marine C:N:P stoichiometry: can the composition of seston explain stable Redfield ratios? *Biogeosciences* **8**, 2917–2933 (2011).
- Tanioka, T., Ficht, C. & Matsumoto, K. Toward determining the spatio-temporal variability of upper-ocean ecosystem stoichiometry from satellite remote sensing. *Front. Mar. Sci.* **7**, 604893 (2020).
- Talmy, D., Martiny, A., Hill, C., Hickman, A. & Follows, M. Microzooplankton regulation of surface ocean POC:PON ratios. *Glob. Biogeochem. Cycle* **30**, 311–332 (2016).
- Minor, E. C., Eglinton, T. I., Olson, R. & Boon, J. J. The compositional heterogeneity of particulate organic matter from the surface ocean: an



- investigation using flow cytometry and DT-MS. *Org. Geochem.* **29**, 1561 (1998).
18. Baer, S., Lomas, M., Terpis, K., Mougino, C. & Martiny, A. C. Stoichiometry of *Prochlorococcus*, *Synechococcus*, and small eukaryotic populations in the western North Atlantic Ocean. *Environ. Microbiol.* **19**, 1568–1583 (2017).
  19. Garcia, C. et al. Nutrient supply controls particulate elemental concentrations and ratios in the low latitude eastern Indian Ocean. *Nat. Commun.* **9**, 4868 (2018).
  20. Casey, J., Aucan, J., Goldberg, S. & Lomas, M. Changes in partitioning of carbon amongst photosynthetic pico- and nano-plankton groups in the Sargasso Sea in response to changes in the North Atlantic Oscillation. *Deep Sea Res. II* **93**, 58–70 (2013).
  21. Martiny, A. C., Vrugt, J. A., Primeau, F. & Lomas, M. Regional variation in the particulate organic carbon to nitrogen ratio in the surface ocean. *Glob. Biogeochem. Cycle* **27**, 23–731 (2013).
  22. Campbell, L., Nolla, H. A. & Vaulot, D. The importance of *Prochlorococcus* to community structure in the central North Pacific Ocean. *Limnol. Oceanogr.* **39**, 955–961 (1994).
  23. Landry, M. R. & Kirchman, D. L. Microbial community structure and variability in the tropical Pacific. *Deep Sea Res. Part II-Top. Stud. Oceanogr.* **49**, 2669–2693 (2002).
  24. Haldal, M., Scanlan, D. J., Norland, S., Thingstad, F. & Mann, N. H. Elemental composition of single cells of various strains of marine *Prochlorococcus* and *Synechococcus* using X-ray microanalysis. *Limnol. Oceanogr.* **48**, 1732–1743 (2003).
  25. Fuhrman, J. A., Sleeter, T. D., Carlson, C. A. & Proctor, L. M. Dominance of bacterial biomass in the Sargasso sea and its ecological implications. *Mar. Ecol. Prog. Ser.* **57**, 207–217 (1989).
  26. Ho, T. et al. The elemental composition of some marine phytoplankton. *J. Phycol.* **39**, 1145–1159 (2003).
  27. Whitney, L. P. & Lomas, M. W. Growth on ATP elicits a P-stress response in the picoeukaryote *Micromonas pusilla*. *PLoS ONE* **11**, e0155158 (2016).
  28. Whitney, L. P. & Lomas, M. W. Phosphate utilization by eukaryotic phytoplankton. *Limnol. Oceanogr. Lett.* **4**, 18–24 (2019).
  29. Hartmann, M. et al. Efficient CO<sub>2</sub> fixation by surface *Prochlorococcus* in the Atlantic Ocean. *ISME J.* **8**, 2280–2289 (2014).
  30. Cailliau, C., Claustre, H., Vidussi, F., Marie, D. & Vaulot, D. Carbon biomass, and gross growth rates as estimated from C-14 pigment labelling, during photoacclimation in *Prochlorococcus* CCMP 1378. *Mar. Ecol. Prog. Ser.* **145**, 209–221 (1996).
  31. Moore, L. R. & Chisholm, S. W. Photophysiology of the marine cyanobacterium *Prochlorococcus*: ecotypic differences among cultured isolates. *Limnol. Oceanogr.* **44**, 628–638 (1999).
  32. Moore, L. R., Goericke, R. & Chisholm, S. W. Comparative physiology of *Synechococcus* and *Prochlorococcus* - influence of light and temperature on growth, pigments, fluorescence and absorptive properties. *Mar. Ecol. Prog. Ser.* **116**, 259–275 (1995).
  33. Kana, T. M., Feiwel, N. L. & Flynn, L. C. Nitrogen starvation in marine *Synechococcus* strains: clonal differences in phycobiliprotein breakdown and energy coupling. *Marine Ecol.* **88**, 75–82 (1992).
  34. Green, B. R. What happened to the phycobilisome? *Biomolecules* **9**, <https://doi.org/10.3390/biom9110748> (2019).
  35. Stadnichuk, I. N. & Tropin, I. V. Antenna replacement in the evolutionary origin of chloroplasts. *Microbiology* **83**, 299–314 (2014).
  36. Boyd, P. W., others, a. Marine phytoplankton temperature versus growth responses from polar to tropical waters, outcome of a scientific community-wide study. *PLoS ONE* **8**, e63091 (2013).
  37. Raven, J. A. & Geider, R. J. Temperature and algal growth. *New Phytologist* **110**, 441–461 (1988).
  38. Fu, F. X., Warner, M. E., Zhang, Y., Feng, Y. & Hutchins, D. A. Effects of increased temperature and CO<sub>2</sub> on photosynthesis, growth, and elemental ratios in marine *Synechococcus* and *Prochlorococcus* (Cyanobacteria). *J. Phycol.* **43**, 485–496 (2007).
  39. Martiny, A. C., Ma, L. Y., Mougino, C., Chandler, J. W. & Zinser, E. R. Interactions between thermal acclimation, growth rate, and phylogeny influence *Prochlorococcus* elemental stoichiometry. *PLoS ONE* **11**, <https://doi.org/10.1371/journal.pone.0168291> (2016).
  40. Szul, M. J., Dearth, S. P., Campagna, S. R. & Zinser, E. R. Carbon fate and flux in *Prochlorococcus* under nitrogen limitation. *mSystems* **4**, e00254–00218 (2019).
  41. Van Mooy, B. A. S. et al. Phytoplankton in the ocean use non-phosphorus lipids in response to phosphorus scarcity. *Nature*, <https://doi.org/10.1038/nature07659> (2009).
  42. Eppley, R. W. Temperature and phytoplankton growth in the sea. *Fish. Bull.* **70**, 1063–1085 (1972).
  43. Garcia, N. et al. High variability in cellular stoichiometry of carbon, nitrogen, and phosphorus within classes of marine eukaryotic phytoplankton under sufficient nutrient conditions. *Front. Microbiol.* **9**, 543 (2018).
  44. Yvon-Durocher, G., Dossena, M., Trimmer, M., Woodward, G. & Allen, A. P. Temperature and the biogeography of algal stoichiometry. *Glob. Ecol. Biogeogr.* **24**, 562–570 (2015).
  45. Toseland, S. et al. The impact of temperature on marine phytoplankton resource allocation and metabolism. *Nat. Clim. Change* **3**, 979–984 (2013).
  46. Geider, R. J. & LaRoche, J. Redfield revisited: variability of C:N:P in marine microalgae and its biochemical basis. *Eur. J. Phycol.* **37**, 1–17 (2002).
  47. Baer, S. E. et al. Carbon and nitrogen productivity during spring in the oligotrophic Indian Ocean along the GO-SHIP IO9N transect. *Deep Sea Res. II*, 81–91 (2019).
  48. Cullen, J. & Eppley, R. W. Chlorophyll maximum layers of the South California Bight and possible mechanisms of their formation and maintenance. *Oceanol. Acta* **4**, 23–32 (1981).
  49. Rhee, G. Y. & Gotham, I. J. The effect of environmental factors on phytoplankton growth: temperature and the interactions of temperature with nutrient limitation. *Limnol. Oceanogr.* **26**, 635–648 (1981).
  50. Saito, M. A., Goepfert, T. J. & Ritt, J. T. Some thoughts on the concept of colimitation: three definitions and the importance of bioavailability. *Limnol. Oceanogr.* **53**, 276–290 (2008).
  51. Edwards, K. F. Mixotrophy in nanoflagellates across environmental gradients in the ocean. *Proc. Acad. Nat. Sci. Phila.* **116**, 6211–6220 (2019).
  52. Zubkov, M. V. & Tarran, G. A. High bacterivory by the smallest phytoplankton in the North Atlantic Ocean. *Nature* **455**, 224–226 (2008).
  53. Bertilsson, S., Berglund, O., Pullin, M. & Chisholm, S. W. Release of dissolved organic matter by *Prochlorococcus*. *Vie Et Milieu* **55**, 225–231 (2005).
  54. Ammerman, J. W., Hood, R. R., Case, D. & Cotner, J. B. Phosphorus deficiency in the Atlantic: an emerging paradigm in oceanography. *EOS* **84**, 165–170 (2003).
  55. Lomas, M. W. et al. Sargasso Sea phosphorus biogeochemistry: an important role for dissolved organic phosphorus (DOP). *Biogeosciences* **7**, 695–710 (2010).
  56. Wu, J., Sunda, W., Boyle, E. & Karl, D. Phosphate depletion in the western North Atlantic Ocean. *Science* **289**, 759–762 (2000).
  57. van Mooy, B. A. S. & Devol, A. H. Assessing nutrient limitation of *Prochlorococcus* in the North Pacific subtropical gyre by using an RNA capture method. *Limnol. Oceanogr.* **53**, 78–88 (2008).
  58. Garcia, N., Bonachela, J. A. & Martiny, A. C. Interactions between growth-dependent changes in cell size, nutrient supply and cellular elemental stoichiometry of marine *Synechococcus*. *ISME Journal* **10**, 2715–2724 (2016).
  59. Kashtan, N. et al. Single cell genomics reveals hundreds of coexisting subpopulations in wild *Prochlorococcus*. *Science* **344**, 416–420 (2014).
  60. Pitt, F. et al. A sample-to-sequence protocol for genus targeted transcriptomic profiling: application to marine *Synechococcus*. *Front. Microbiol.* **7**, <https://doi.org/10.3389/fmicb.2016.01592> (2016).
  61. Lomas, M. W. & Martiny, A. C. Direct measure of phytoplankton cell quotas from field populations sampled from multiple cruises between 2010 and 2016. Biological and Chemical Oceanography Data Management Office (BCO-DMO). (Version 1) Version Date 2021-06-02. <https://doi.org/10.26008/21912/bco-dmo.849153.849151> (2021).
  62. Gordon, L., Jennings, J., Jr., Ross, A. & Krest, J. A suggested protocol for continuous flow automated analysis of seawater nutrients (phosphate, nitrate, nitrite, and silicic acid) in the WOCE Hydrographic Program and the Joint Global Ocean Fluxes Study, 55 (Oregon State University, 1993).
  63. Hydes, D. J. et al. Determination of dissolved nutrients (N, P, Si) in seawater with high precision and inter-comparability using gas-segmented continuous flow analyzers. IOCCP Report No. 14, 87 (2010).
  64. Knap, A. et al. BATS Methods Manual Version 4. (U.S. JGOFS Planning Office, Woods Hole, 1997).
  65. Karl, D. M. & Tien, G. MAGIC: A sensitive and precise method for measuring dissolved phosphorus in aquatic environments. *Limnol. Oceanogr.* **37**, 105–116 (1992).
  66. Rimmelin, P. & Moutin, T. Re-examination of the MAGIC method to determine low orthophosphate concentration in seawater. *Anal. Chim. Acta* **548**, 174–182 (2005).

## Acknowledgements

We thank the Captains and crews of the various vessels that supported these sea-going efforts. We thank Agathe Talarmin for sorting samples collected from the SPOTS time-series and the Newport Pier. We thank Damian Grundle for inviting MWL on the Sonne 243 cruise to collect samples in the Peru upwelling system. We acknowledge the National Science Foundation for supporting our research (OCE-1046297, OCE-1559002, and OCE-1848576 to ACM and OCE-1045966, OCE-1756054, and OCE-1756271 to MWL).

## Author contributions

M.W.L. and A.C.M. conceived the original idea. M.W.L. wrote the manuscript and prepared the figures with feedback and reviews from other authors. S.E.B., C.M., K.X.T.,

D.A.L. and M.A.A. all contributed to the at-sea collection and/or laboratory analysis of samples presented in this manuscript.

### Competing interests

The authors declare no competing interests.

### Additional information

**Supplementary information** The online version contains supplementary material available at <https://doi.org/10.1038/s43247-021-00212-9>.

**Correspondence** and requests for materials should be addressed to M.W.L.

**Peer review information** Communications Earth & Environment thanks the anonymous reviewers for their contribution to the peer review of this work. Primary Handling Editors: Clare Davis.

**Reprints and permission information** is available at <http://www.nature.com/reprints>

**Publisher's note** Springer Nature remains neutral with regard to jurisdictional claims in published maps and institutional affiliations.



**Open Access** This article is licensed under a Creative Commons Attribution 4.0 International License, which permits use, sharing, adaptation, distribution and reproduction in any medium or format, as long as you give appropriate credit to the original author(s) and the source, provide a link to the Creative Commons license, and indicate if changes were made. The images or other third party material in this article are included in the article's Creative Commons license, unless indicated otherwise in a credit line to the material. If material is not included in the article's Creative Commons license and your intended use is not permitted by statutory regulation or exceeds the permitted use, you will need to obtain permission directly from the copyright holder. To view a copy of this license, visit <http://creativecommons.org/licenses/by/4.0/>.

© The Author(s) 2021